Polymeric semiconductor/graphene hybrid field-effect transistors

Jia Huang [a,b,*], Daniel R. Hines [a], Byung Jun Jung [e], Merijntje S. Bronsgeest [a,b], Andrew Tunnell [a,b], Vince Ballarotto [a], Howard E. Katz [d], Michael S. Fuhrer [b], Ellen D. Williams [a,b], John Cumings [a,b,c,*]

[a] Laboratory for Physical Sciences, College Park, MD 20742, USA
[b] Center for Nanophysics and Advanced Materials, University of Maryland, College Park, MD 20742, USA
[c] Department of Materials Science and Engineering, University of Maryland, College Park, MD 20742, USA
[d] Department of Materials Science and Engineering, Johns Hopkins University, Baltimore, MD 21218, USA
[e] Department of Materials Science and Engineering, The University of Seoul, Seoul 130-742, Republic of Korea

ARTICLE INFO

ABSTRACT

Solution processed organic field-effect transistors (OFETs) usually have high on/off ratios but suffer from low mobilities, while transistors based on graphene usually exhibit very high mobilities but low on/off ratios. We demonstrate a straightforward route to solve the challenging problem of enhancing the effective mobility in OFETs while keeping the on/off ratio sufficiently high. We achieve this by developing hybrid FETs incorporating both organic semiconductors and graphene. Compared against OFETs with only pure organic semiconductors, our hybrid FETs exhibit up to 20 times higher effective mobilities, and yet they keep the on/off ratios comparable or better. P3HT/graphene hybrid FETs exhibit mobility as high as $0.17 \text{ cm}^2 \text{ V}^{-1} \text{ s}^{-1}$, and PQT-12/graphene hybrid FETs show effective mobility up to $0.6 \text{ cm}^2 \text{ V}^{-1} \text{ s}^{-1}$. We expect that incorporating graphene is a general route to enhance the performance of OFETs, providing a low-cost avenue for enhancing OFET performance.

1. Introduction

Organic and polymeric semiconductors offer potential low-cost, high-volume manufacturing of flexible transistor-based electronics, such as display drivers, radio frequency identification tags, pressure mapping elements, and chemical sensors [1–8]. These materials typically exhibit high on/off ratios in organic field-effect transistors (OFETs), but suffer from low mobilities that limit the range of possible applications [9,10]. Although tremendous progress has been made in improving mobility through developing new materials and novel process techniques, the need for higher mobility organic semiconductors is still compelling, especially for materials used in conjunction with solution processes. In contrast to these organic semiconductor materials, carbon-based materials such as graphene and carbon nanotubes (CNTs) exhibit very high mobility but usually suffer from low on/off ratio in field-effect transistors (FETs) [11–13]. With the aim of enhancing the effective mobility in OFETs while keeping the on/off ratio sufficiently high, we have developed composite thin-films containing both organic semiconductor materials and graphene flakes.

There have been a few studies dealing with organic semiconductor/carbon nanotube hybrid field-effect transistors [14–19], which have reported a remarkable increase in apparent field-effect mobility resulting from CNTs having been inserted into or beneath the semiconductor film. These studies suggest that CNTs act as conducting bridges between the crystalline regions of the semiconductor film. However, the on/off ratio appears to decrease just as the mobility begins to increase. This is because one-dimensional carbon nanotubes start to percolate at low

* Corresponding authors. Addresses: Center for Nanophysics and Advanced Materials, University of Maryland, College Park, MD 20742, USA. Tel.: +1 443 610 4174 (J. Huang), Department of Materials Science and Engineering, University of Maryland, College Park, MD 20742, USA. Tel.: +1 301 405 0789; fax: +1 301 314 8164 (J. Cumings).

E-mail addresses: jhuang17@umd.edu (J. Huang), cumings@umd.edu (J. Cumings).

density; when there are enough carbon nanotubes mixed into the organic semiconductor film to drastically enhance mobility, the density of the CNTs appears to approach the percolation threshold, thus limiting the maximum mobility achievable before the percolation of CNT reduces the on/off ratio of such a hybrid organic/CNT transistor. Graphene, a two-dimensional lattice of carbon with single atom thickness, has generated significant attention due to its outstanding electronic, mechanical and physical properties [13]. As with the addition of CNTs, it is expected that few-layer and single-layer graphene flakes can provide good connection between the crystalline regions of the semiconductor film. Compare to CNTs, increased area in the conduction channel of an organic semiconductor transistor can be covered by graphene flakes before they start to percolate and reduce the on/off ratio. As a result, the mobility of organic transistors with graphene flakes would be expected to show higher values than what can be accomplished using CNTs before device on/off ratio drops.

Recent progress with liquid exfoliation of graphene provides cost efficient methods to prepare graphene dispersions [20–22]. Coleman et al. first reported the exfoliation of graphene in N-methyl-2-pyrrolidone (NMP) [20], and then the Tour and Barron groups reported exfoliation of graphene in ortho dichlorobenzene (ODCB) with higher graphene concentration [21]. In our method, graphite was exfoliated in ODCB. Not only is ODCB a good solvent for organic semiconductors, but also graphene flakes can be dispersed in ODCB without the aid of surfactants. Therefore ODCB appears to be a good solvent for hybrid organic semiconductor/graphene films. In this paper, we present a general approach for the preparation of solution processable organic semiconductor/graphene hybrid thin film transistors. Compared to FETs with pure organic semiconductors, hybrid FETs exhibit much higher effective mobility while keeping the on/off ratio of devices sufficiently high.

2. Materials and methods

In this work, poly(3,3-didodecylquaterthiophene) (PQT-12) was chosen as the organic semiconductor material because of its good air stability. Additionally, poly-(3-hexylthiophene) (P3HT), an organic semiconductor widely used for both organic transistor and organic photovoltaic device studies, was also studied to prove that our method is a general route to enhance the performance of polymer transistors.

We synthesized PQT-12 according to FeCl$_3$-mediated oxidative coupling polymerization [25]. Our PQT-12 showed almost the same thermal behavior in the differential scanning calorimetry (DSC) thermogram with Xerox's PQT-12 [26,27]. Regioregular P3HT (94.5%, M_n = 13,000 and M_w = 26,200 g/mol) was purchased from Merck and used without further purification. Graphene dispersions were prepared by an adaptation of the solution sonication method reported previously by the Tour and Barron groups [21]. Briefly, graphite (Asbury Graphite Mills Inc.) was added into ODCB at a concentration of 5 mg/ml. The mixture was then sonicated for 45 min with an ultrasonicator

(Heilscher 400) at 50% power. After ultrasonication, graphene dispersions were left to settle for about 1 h to allow thick graphite flakes to sediment out of solution. The top portion of the solution was then centrifuged at 1500 rpm for 1 h. The supernatant from the top half of the solution yielded a graphene dispersion which contained single-layered and multi-layered graphene flakes. Three milligrams of PQT-12 or P3HT was then added to 1 ml of this graphene dispersion. The mixture was heated to allow the polymer to dissolve completely. The hot solution was then subjected to ultrasonic agitation and cooled to room temperature [24]. This yielded a dark-purple solution with polymer nanoparticles and graphene flakes suspended in ODCB. A heavily doped silicon wafer with 300 nm thermally grown SiO$_2$ was used as a substrate material. Wafers were cleaned by sonication in acetone, isopropanol and DI water, respectively, followed by N$_2$ drying. Some of the substrates were used as cleaned, while others were treated with an octyltrichlorosilane (OTS-8) self-assembled monolayer (SAM). OTS-8 self-assembled monolayer was deposited on a wafer surface by immersion into a 10 mM solution of OTS-8 in toluene at 60 °C for 15 min, subsequent rinsing with toluene and ethanol, and then blow-drying with nitrogen before use [24]. Hybrid field-effect transistors were fabricated by spin coating the PQT-12/graphene (or P3HT/graphene) composite solution onto a substrate at 1200 rpm for 60 s followed by vacuum drying to give 20–50-nm thick semiconductor layer. Control devices were fabricated with pure PQT-12 (or P3HT) films using the same procedures but without the addition of graphene flakes to the ODCB solution. Following deposition of the organic semiconductor films, gold source-drain electrodes were deposited by thermal evaporation through a shadow mask with channel length L = 130 μm and channel width W = 2 mm. As indicated in the text, some of the resulting devices were annealed in a vacuum oven at 140 °C for 20 min, followed by slow cooling.

All the current–voltage (I–V) curves were measured at room temperature under ambient conditions using a Cascade probe station connected to two Keithley 2400 source/measure units. The effective field-effect mobility of each transistor was extracted from the transfer characteristics using a linear fit to the plot of the square root of saturation source-drain current as a function of the gate voltage V_g.

3. Results and discussion

The concentration of graphene in the hybrid films was measured by two methods. First, graphene dispersion with known volume was slowly dropped onto a heated glass slide. After complete solvent evaporation, the mass change of the glass slide was carefully measured. With this method, the concentration of graphene in the dispersion was calculated to be about 0.055 mg/ml. In another method, the graphene concentration was determined by UV–vis–IR absorption spectroscopy (see Supplementary data). The spectra are featureless in the visible–IR region as expected [23]. An average absorption coefficient for graphene of 2460 L/g m at a wavelength of 660 nm was
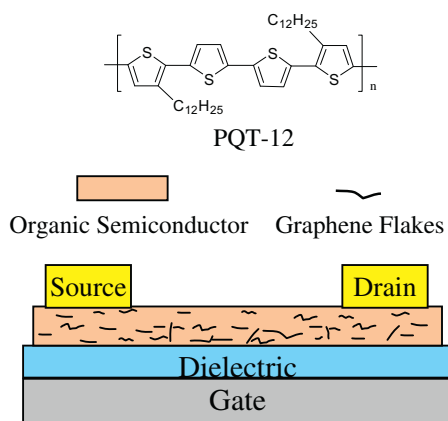
C12H25

PQT-12

Organic Semiconductor   Graphene Flakes

Source | Drain
Dielectric
Gate

Fig. 1. Structure of organic semiconductor/graphene hybrid FET.

used for the calculation [20]. Therefore, optical methods can be employed to measure the concentration of graphene which was calculated to be about 0.045 mg/ml in the deposition dispersion. The first method gives a slightly higher concentration, which is believed to be due to the residual decomposed ODCB solvent on the heated glass slide.

As shown in Fig. 1, graphene flakes incorporated into an organic semiconductor film is expected to provide "fast lanes" for charge carriers within the conduction channel, enhancing the effective mobility of the entire transistor device. That is, the addition of graphene flakes might effectively reduces the conduction channel length, which acts to enhance the output source-drain current of the field-effect transistor. This activity is realized in the ambient laboratory atmosphere.

Transistors with and without substrate surface treatment or post-fabrication annealing process were all studied. For transistors fabricated without any substrate surface treatment or post annealing process, PQT-12/graphene hybrid FETs exhibited source-drain current about 10 times higher than that of a control device (containing only PQT-12 with no added graphene). Fig. 2 compares I–V characteristics of a control device and a PQT-12/graphene hybrid transistor both on a cleaned SiO_2 surface without any customized surface treatment. The mobility of the

control device is 0.012 cm^2 V^{-1} s^{-1}, while the mobility of the PQT-12/graphene hybrid FET is 0.17 cm^2 V^{-1} s^{-1}. The on/off ratios of both devices are on the order of 10^3 but better on/off ratios could be achieved by post-fabrication annealing the devices as described below.

When substrate surface treatment and post-fabrication annealing process are performed, both PQT-12/graphene hybrid FETs and control devices exhibit better performance, but PQT-12/graphene hybrid FETs show significantly greater enhancement. Fig. 3 shows source-drain I–V curves and transfer curves for both control devices and hybrid FETs fabricated on substrate surfaces that were treated with octyltrichorosilane (OTS-8) and were vacuum annealed after fabrication. The effective mobility of the control device is 0.15 cm^2 V^{-1} s^{-1}, which is comparable to previously reported values [24]. In contrast, the effective mobility of the PQT-12/graphene hybrid FET is 0.55 cm^2 V^{-1} s^{-1}, which is remarkably high for a PQT-12 FET. In comparison, the highest prior report mobility for pure PQT-12 is 0.2 cm^2 V^{-1} s^{-1} [24]. The on/off ratio of both devices are as high as 10^5 with the off current on the order 10^{-9} A when measured in air after vacuum annealing. The low off current obtained suggests that densities of graphene flakes in these PQT-12/graphene hybrid films are still lower than the percolation threshold of graphene.

To study the dependence of device performance on graphene dispersion concentration, hybrid PQT-12/graphene films containing higher densities of graphene flakes were also studied. Graphene dispersions at higher concentration can be prepared by first preparing graphene dispersion according to procedures described in Section 2, followed by removing some of the ODCB solvent either by rotary evaporation or by rapid heating in a shallow poly(tetrafluroethylene) (PTFE) dish. These high-concentration graphene dispersions are then mixed with PQT-12 semiconductor and deposited on substrates. It should be noted that if the graphene dispersion is heated in air for a long time (more than 10 min), graphene flakes will start to aggregate and precipitate, probably due to the adsorption of water into solution. This can be avoided by using a shallow dish with large surface area to reduce the time needed for the graphene dispersion to be exposed to air, or using a rotary evaporator to exclude water during the process. Sometimes during concentration, a small
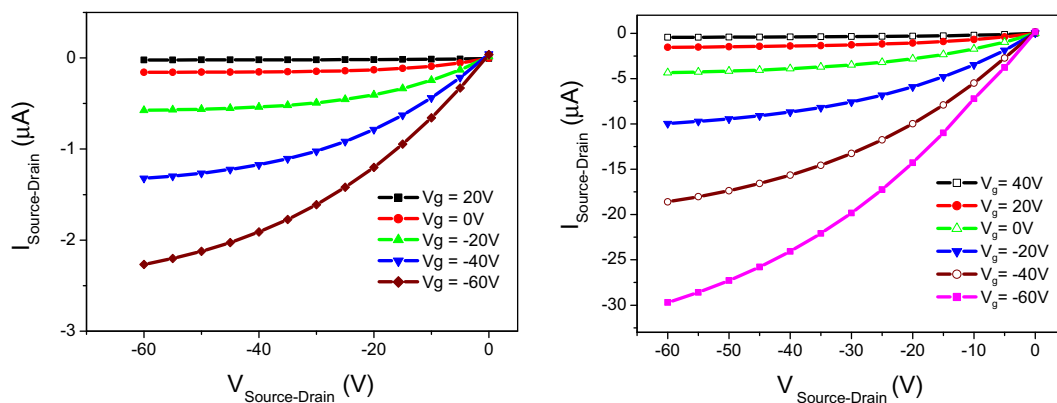

Fig. 2. Source-drain I–V curves of a pure PQT-12 FET (left) and a PQT-12/graphene hybrid FET (right).
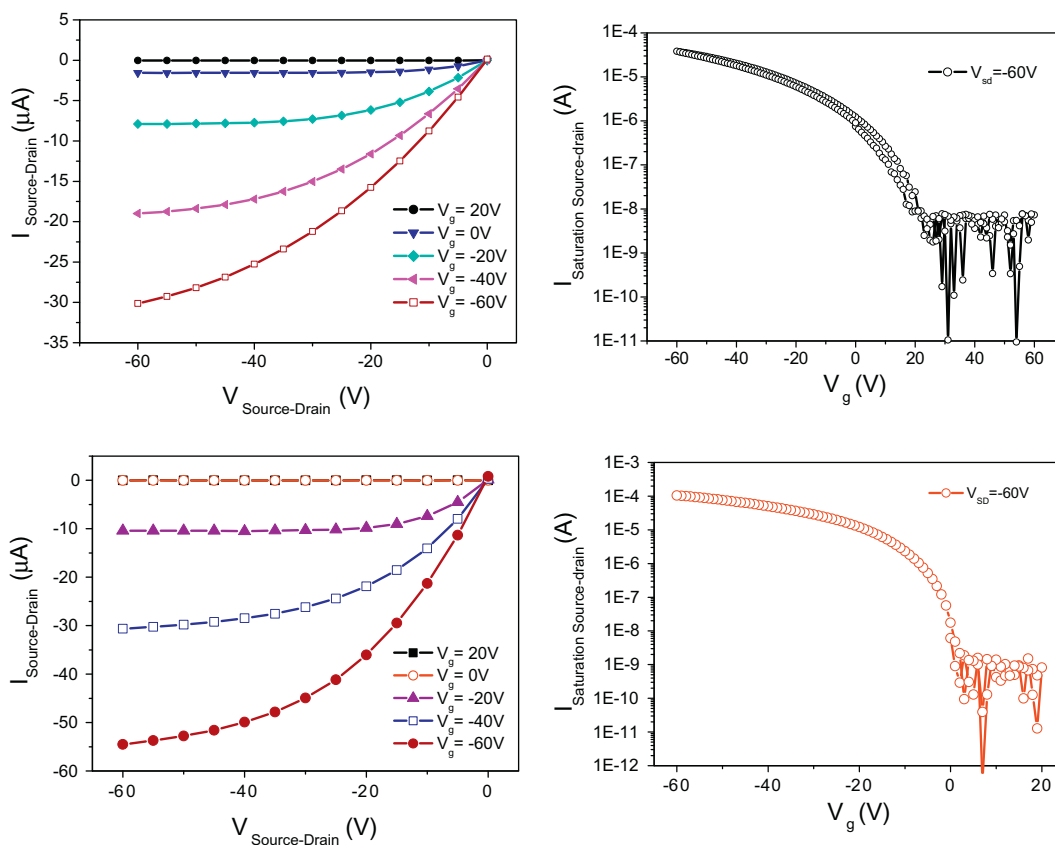
Fig. 3. Source-drain I–V curve (left) and transfer curve (right) of a PQT-12 FET (top) and a PQT-12/graphene hybrid FET (bottom) with OTS-8 surface treatment and vacuum annealing.

amount of graphene precipitates out, but can be re-dispersed into suspension by ultrasonication for 5 min. The resulting ink-like graphene dispersions at higher concentrations are only stable for a short time, and hence should be used right after preparation. For this study, graphene dispersions concentrated by 4 times and 10 times were prepared and mixed with PQT-12 semiconductor immediately after graphene dispersion preparation, followed by 5 min sonication. Hybrid transistors were then fabricated using these organic semiconductor/graphene composite solutions according to the same procedures as described above and are referred to below as PQT-12/4× graphene FETs and PQT-12/10× graphene FETs, respectively.

Fig. 4 summarizes the maximum mobilities, average mobilities and on/off ratios of all transistors measured. Error bars in the figure show the highest mobilities measured for each type of device, while the columns show averaged values. Field-effect transistors fabricated from 4× concentrated graphene dispersions exhibited average mobility of 0.32 $cm^2 V^{-1} s^{-1}$, which is lower than that of devices made from graphene dispersion at normal concentration. This is probably due to the fact that, when too many graphene flakes are present in PQT-12 film, the structural order in the PQT-12 is decreased. This is supported by X-ray diffraction results showing a loss of crystallinity with increasing graphene concentration, as
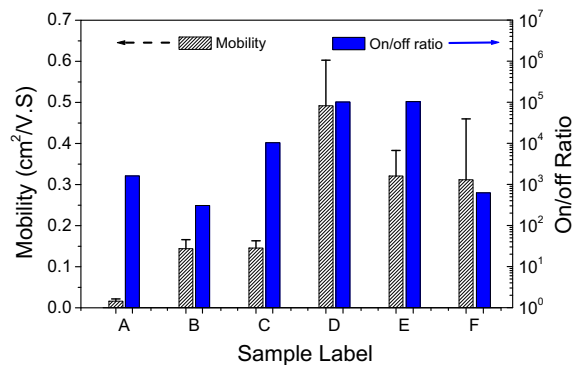

Fig. 4. Summary of mobilities and on/off ratio of all PQT-12 transistors with/without graphene: (A) PQT-12 FET no OTS8 and no annealing. (B) PQT-12/graphene FET no OTS-8 and no annealing. (C) PQT-12 FET with OTS-8 and annealing. (D) PQT-12/graphene FET with OTS-8 and annealing. (E) PQT-12/4×-graphene FET with OTS and annealing. (F) PQT-12/10×-graphene FET with OTS and annealing.

shown in the Supplementary data. Although more graphene flakes can provide more "fast lanes" for charge carriers in conduction channels, more disordered PQT-12 semiconductor layers ultimately reduce the effective mobility of devices. At this concentration, the density of graphene flakes in polymer is believed to be still lower than the percolation threshold, so that the on/off ratios of
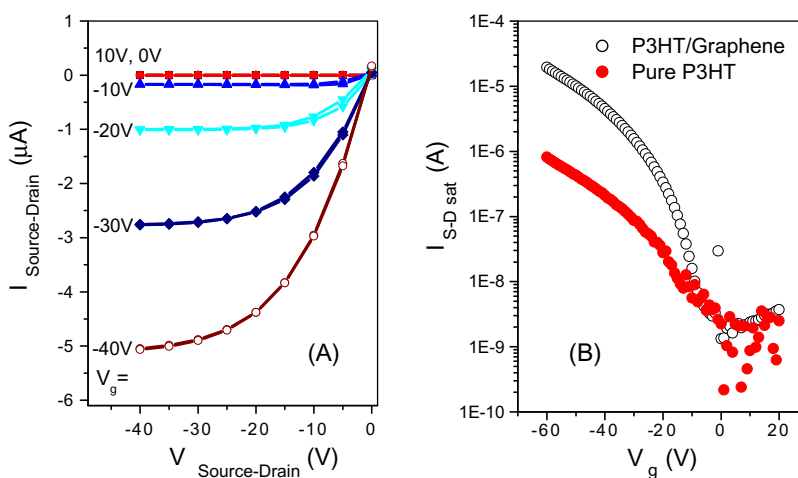
Fig. 5. (A) Source-drain *I–V* curve of a P3HT/graphene hybrid FET. (B) Transfer characteristics of pure P3HT and P3HT/graphene hybrid FET.

PQT-12/4× graphene FETs remain in the same order of magnitude as transistors with regular graphene concentration. However, when 10 times concentrated graphene dispersion was added into PQT-12 semiconductor, the on/off ratio of transistors was decreased significantly, suggesting that the density of graphene flakes in the polymer exceeds the percolation threshold. Off currents of these PQT-12/10× graphene FETs are on the order of 10^{-7} A, hundreds of times higher than that of PQT-12/graphene FETs with graphene dispersion at normal concentration.

Additionally, P3HT was also studied to demonstrate that our approach is a general route to enhance the performance of transistors made from polymer semiconductors. P3HT/graphene hybrid FETs were fabricated using the same methods on OTS-8 treated substrates, and again, all devices were fabricated and measured under ambient conditions. The measured current–voltage characteristics for P3HT/graphene FETs show well-defined gate modulation. As an example, Fig. 5A depicts the current–voltage characteristics of a P3HT/graphene FET, and Fig. 5B compares the transfer characteristics of a P3HT/graphene hybrid transistor to that of a pure P3HT FET. As can be seen, much higher current was obtained from the device with graphene. The P3HT/graphene FET exhibits mobility as high as 0.17 cm^2 V^{-1} s^{-1}, which is more than 20 times higher than that from the pure P3HT FET (0.007 cm^2 V^{-1} s^{-1}). The on/off ratio of the P3HT/graphene FET is on the order of 10^4, which is surprisingly an order of magnitude *higher* than that of the pure P3HT FET in contrast to what is observed in P3HT/carbon-nanotube composites. [14] This is because both devices exhibit similar off currents, while the P3HT/graphene FET shows much higher on current. These results suggest that our method is a general route to enhance the performance of polymer electronics.

4. Conclusions

In conclusion, we have developed composite field-effect transistors containing both polymer semiconductor

materials and graphene flakes, and we have shown that effective mobilities of polymer/graphene hybrid FETs can be significantly higher than that of a pure polymer FET. When graphene dispersions with concentrations at about 0.05 mg/ml are mixed with PQT-12 semiconductor, effective mobilities as high as 0.5 ± 0.1 cm^2 V^{-1} s^{-1} can be obtained in ambient conditions, while the on/off ratio of these devices can be on the order of 10^5 and was not reduced due to the addition of graphene flakes. This is attributed to the high percolation threshold of graphene. When the concentration of graphene flakes in the semiconductor film was increased by 4 times, the effective mobility was decreased to 0.32 ± 0.06 cm^2 V^{-1} s^{-1} because the high density graphene flakes in the organic semiconductor layer probably resulted in a more disordered film. The on/off ratio of hybrid FETs significantly decreased when the concentration of graphene flakes in semiconductor film was increased by 10 times, which is believed to exceed the percolation threshold of graphene flakes. We also found that effective mobilities of P3HT/graphene hybrid FETs can be more than 20 times higher than that of pure P3HT FETs we fabricated. We expect that adding graphene flakes to organic semiconductors is a general route to enhance the performance of organic electronics, providing a low-cost avenue for enhancing OFET performance.

Appendix A. Supplementary data

Supplementary data associated with this article can be found, in the online version, at doi:10.1016/j.orgel.2011.05.021.

References

[1] S.E. Burns, K. Reynolds, W. Reeves, M. Banach, T. Brown, K. Jacobs, A. Menon, S. Siddique, P. Too, C. Ramsdale, J. Watts, P. Cain, T. von Werne, J. Mills, C. Curling, H. Sirringhaus, K. Amindson, M.D. McCreary, J. Soc. Inf. Display 13 (2005) 583.
[2] T.W. Kelley, P.F. Baude, C. Gerlach, D.E. Ender, D. Muyres, M.A. Haase, D.E. Vogel, S.D. Theiss, Chem. Mater. 16 (2004) 4413.
[3] J. Huang, J. Miragliotta, A. Becknell, H.E. Katz, J. Am. Chem. Soc. 129 (2007) 9366.
[4] T. Someya, A. Dodabalapur, J. Huang, K.C. See, H.E. Katz, Adv. Mater. 22 (2010) 3799.
[5] J. Huang, T.J. Dawidcyk, B.J. Jung, J. Sun, A.F. Mason, H.E. Katz, J. Mater. Chem. 20 (2010) 2644.
[6] H.E. Katz, J. Huang, Annu. Rev. Mater. Res. 39 (2009) 71.
[7] J. Huang, J. Sun, H.E. Katz, Adv. Mater. 20 (2008) 2567.
[8] R. Parashkov, E. Becker, T. Riedel, H.H. Johannes, W. Kowalsky, Proc. IEEE 93 (2005) 1321.
[9] C. Reese, M. Roberts, M.M. Ling, Z. Bao, Mater. Today 7 (2004) 20.
[10] A. Salleo, Mater. Today 10 (2007) 38.
[11] M.S. Fuhrer, B.M. Kim, T. Durkop, T. Brintlinger, Nano Lett. 2 (2002) 755.
[12] E.S. Snow, J.P. Novak, P.M. Campbell, D. Park, Appl. Phys. Lett. 82 (2003) 145.
[13] A.K. Geim, K.S. Novoselov, Nat. Mater. 6 (2007) 183.
[14] X.Z. Bo, C.Y. Lee, M.S. Strano, M. Goldfinger, C. Nuckolls, G.B. Blanchet, Appl. Phys. Lett. 86 (2005) 182102.
[15] X.Z. Bo, N.G. Tassi, C.Y. Lee, M.S. Strano, C. Nuckolls, G.B. Blanchet, Appl. Phys. Lett. 87 (2005) 203510.
[16] J.X. Geng, B.S. Kong, S.B. Yang, S.C. Youn, S. Park, T. Joo, H.T. Jung, Adv. Funct. Mater. 18 (2008) 2659.
[17] S. Liu, S.C.B. Mannsfeld, M.C. LeMieux, H.W. Lee, Z. Bao, Appl. Phys. Lett. 92 (2008) 053306.
[18] Y.D. Park, J.A. Lim, Y. Jang, M. Hwang, H.S. Lee, D.H. Lee, H.J. Lee, J.B. Baek, K. Cho, Org. Electron. 9 (2008) 317.
[19] G.W. Hsieh, F.M. Li, P. Beecher, A. Nathan, Y. Wu, B.S. Ong, W.I. Milne, J. Appl. Phys. 106 (2009) 123706.
[20] Y. Hernandez, V. Nicolosi, M. Lotya, F.M. Blighe, Z.Y. Sun, S. De, I.T. McGovern, B. Holland, M. Byrne, Y.K. Gun'ko, J.J. Boland, P. Niraj, G. Duesberg, S. Krishnamurthy, R. Goodhue, J. Hutchison, V. Scardaci, A.C. Ferrari, J.N. Coleman, Nat. Nanotechnol. 3 (2008) 563.
[21] C.E. Hamilton, J.R. Lomeda, Z.Z. Sun, J.M. Tour, A.R. Barron, Nano Lett. 9 (2009) 3460.
[22] A.A. Green, M.C. Hersam, Nano Lett. 9 (2009) 4031.
[23] D.S.L. Abergel, V.I. Fal'ko, Phys. Rev. B 75 (2007) 155430.
[24] B.S. Ong, Y.L. Wu, P. Liu, S. Gardner, Adv. Mater. 17 (2005) 1141.
[25] B.S. Ong, Y.L. Wu, P. Liu, S. Gardner, J. Am. Chem. Soc. 126 (2004) 3378.
[26] N. Zhao, G.A. Botton, S.P. Zhu, A. Duft, B.S. Ong, Y.L. Wu, P. Liu, Macromolecules 37 (2004) 8307.
[27] J. Sun, B.J. Jung, T. Lee, L. Berger, J. Huang, Y. Liu, D.H. Reich, H.E. Katz, ACS Appl. Mater. Interfaces 1 (2009) 412.